
UMR-MEC Conference on Energy / UMR-DNR Conference on Energy


12 Oct 1978

Concentration of Solar Energy Using a Cassegrain Type Solar Furnace

M. H. Cobble

W. C. Hull

Follow this and additional works at: <https://scholarsmine.mst.edu/umr-mec>

 Part of the [Energy Policy Commons](#), and the [Power and Energy Commons](#)

Recommended Citation

Cobble, M. H. and Hull, W. C., "Concentration of Solar Energy Using a Cassegrain Type Solar Furnace" (1978). *UMR-MEC Conference on Energy / UMR-DNR Conference on Energy*. 389, pp. 348-355.
<https://scholarsmine.mst.edu/umr-mec/389>

This Article - Conference proceedings is brought to you for free and open access by Scholars' Mine. It has been accepted for inclusion in UMR-MEC Conference on Energy / UMR-DNR Conference on Energy by an authorized administrator of Scholars' Mine. This work is protected by U. S. Copyright Law. Unauthorized use including reproduction for redistribution requires the permission of the copyright holder. For more information, please contact scholarsmine@mst.edu.

CONCENTRATION OF SOLAR ENERGY USING A CASSEGRAIN TYPE SOLAR FURNACE

M. H. Cobble and W. C. Hull
New Mexico State University

Abstract

A solar furnace consisting of a paraboloid of revolution that tracks the sun, and a hyperboloid of revolution reflector that has a focus in common with the paraboloid is analyzed using a three-dimensional ray trace to determine the image shape and size, and for the concentration to be obtained for various eccentricities e of the hyperboloid when used with an 84 foot diameter paraboloid (radar dish).

INTRODUCTION

A schematic view of the problem to be considered is shown in Figure 1. The paraboloid tracks the sun, and the sun's image is re-reflected to the hyperboloidal surface, and then re-reflected to the focal plane.

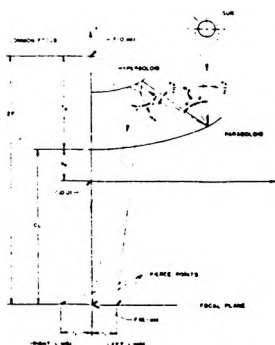


Fig. 1 Cassegrain Geometry

THREE DIMENSIONAL RAY TRACE

Vector \bar{a} , ray from the sun

A ray from any position on the sun may be given as

$$\bar{A} = A_1\bar{i} + A_2\bar{j} + A_3\bar{k} \quad (1)$$

and

$$A = \sqrt{A_1^2 + A_2^2 + A_3^2} \quad (2)$$

so

$$\bar{a} = \frac{\bar{A}}{A} = a_1\bar{i} + a_2\bar{j} + a_3\bar{k} \quad (3)$$

Equation (3) is the normal form of a ray from the sun.

Paraboloid of revolution (concentrator)

The equation of a paraboloid of revolution, see Figure 1, is

$$y = a_0 + \frac{(x^2 + z^2)}{4f_0} \quad (4)$$

where

a_0 = distance from the vertex of the paraboloid to the origin

f_0 = focal length of the paraboloid

and in Figure 1, $r = x^2 + z^2$. We may also write

$$\phi_p = y - \frac{(x^2 + z^2)}{4f_0} = a_0 \quad (5)$$

Normal to the paraboloid, \bar{b}

$$\nabla\phi_p = \frac{\partial\phi_p}{\partial x}\bar{i} + \frac{\partial\phi_p}{\partial y}\bar{j} + \frac{\partial\phi_p}{\partial z}\bar{k} = -\frac{2x}{4f_0}\bar{i} + \bar{j} - \frac{2z}{4f_0}\bar{k}$$

$$= \bar{B} = B_1\bar{i} + B_2\bar{j} + B_3\bar{k} \quad (6)$$

and

where

$$|b| = \begin{vmatrix} b_{11} & b_{12} \\ b_{21} & b_{22} \end{vmatrix}, \quad D_1 = \begin{vmatrix} l_1 & b_{12} \\ l_2 & b_{22} \end{vmatrix},$$

$$D_2 = \begin{vmatrix} b_{11} & l_1 \\ b_{21} & l_2 \end{vmatrix} \quad (30)$$

and where

$$b_{11} = p_1 \quad b_{21} = r_1 \quad l_1 = d_{ab} - p_2 y$$

$$b_{12} = p_3 \quad b_{22} = r_3 \quad l_2 = d_{cp} - r_2 y$$

Thus we can write

$$x = BB_1 + BB_2 y \quad (31)$$

and

$$z = BB_3 + BB_4 y \quad (32)$$

where y is known, or assumed.

Hyperboloid of revolution (cassegain reflector)

The equation for a hyperboloid of revolution, see Figure 1, is

$$\frac{y^2}{a^2} - \frac{(x^2 + z^2)}{b^2} = 1 \quad (33)$$

where

$$F = ae = \frac{1}{2} \text{ distance between foci}$$

and

$$e = \sqrt{\frac{a^2 + b^2}{a^2}} > 1 = \text{eccentricity}$$

So, using Equations (31) and (32), we may write alternately

$$F(y) = \frac{y^2}{a^2} - 1 - \frac{1}{b^2} [(BB_1 + BB_2 y)^2 + (BB_3 + BB_4 y)^2] \quad (34)$$

and

$$F'(y) = \frac{2y}{a^2} - \frac{2}{b^2} [(BB_1 + BB_2 y)BB_2 + (BB_3 + BB_4 y)BB_4] \quad (35)$$

Newton's method

A recursion method for finding y accurately, when an approximate value of y is known, is

$$y_{n+1} = y_n - \frac{F(y_n)}{F'(y_n)} \quad (36)$$

Thus starting with an estimate of y , (y_n), a new value of y , (y_{n+1}), is computed. The process is continued until the difference between y_{n+1} and y_n is as small as desired. Using this method, the coordinates of the pierce point of \bar{c} with the hyperboloid are found, namely (x_1, y_1, z_1) .

Normal to the hyperboloid, \bar{d}

From Equation (33), we may write

$$\begin{aligned} \nabla \phi_n &= \frac{\partial \phi}{\partial x} \bar{i} + \frac{\partial \phi}{\partial y} \bar{j} + \frac{\partial \phi}{\partial z} \bar{k} \\ &= \frac{-2x\bar{i}}{b^2} + \frac{2y\bar{j}}{a^2} - \frac{2z\bar{k}}{b^2} = \bar{D} \\ &= D_1 \bar{i} + D_2 \bar{j} + D_3 \bar{k} \end{aligned} \quad (37)$$

and

$$D = \sqrt{D_1^2 + D_2^2 + D_3^2} \quad (38)$$

so

$$\bar{d} = \frac{\bar{D}}{D} = d_1 \bar{i} + d_2 \bar{j} + d_3 \bar{k} \quad (39)$$

Angle γ between \bar{c} , \bar{d}

From Figure 3, we see that

$$\bar{c} \cdot \bar{d} = cd \cos \gamma = \cos \gamma \quad (40)$$

so

$$\gamma = \cos^{-1} [c_1 d_1 + c_2 d_2 + c_3 d_3] \quad (41)$$

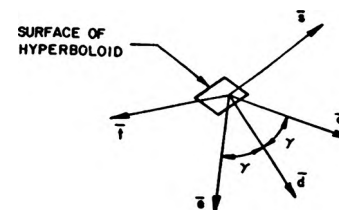


Fig. 3 Vectors at Surface of Hyperboloid

Vector \bar{t} , normal to \bar{c} , \bar{d}

$$\bar{T} = \bar{c} \times \bar{d} = \begin{vmatrix} \bar{i} & \bar{j} & \bar{k} \\ c_1 & c_2 & c_3 \\ d_1 & d_2 & d_3 \end{vmatrix}$$

$$= T_1 \bar{i} + T_2 \bar{j} + T_3 \bar{k} \quad (42)$$

and

$$T = \sqrt{T_1^2 + T_2^2 + T_3^2} \quad (43)$$

so

$$\bar{t} = \frac{\bar{T}}{T} = t_1 \bar{i} + t_2 \bar{j} + t_3 \bar{k} \quad (44)$$

Re-reflected ray \bar{e}

The vector equations for determining \bar{e} are:

$$\bar{d} \cdot \bar{e} = de \cos \gamma = \cos \gamma \quad (45)$$

$$\bar{c} \cdot \bar{e} = ce \cos 2\gamma = \cos 2\gamma \quad (46)$$

$$\bar{t} \cdot \bar{e} = 0 \quad (47)$$

Thus

$$\bar{e} = e_1 \bar{i} + e_2 \bar{j} + e_3 \bar{k} \quad (48)$$

where

$$e_1 = \frac{D_1}{|c|}, \quad e_2 = \frac{D_2}{|c|} \text{ and } e_3 = \frac{D_3}{|c|} \quad (49)$$

and

$$|c| = \begin{vmatrix} c_{11} & c_{12} & c_{13} \\ c_{21} & c_{22} & c_{23} \\ c_{31} & c_{32} & c_{33} \end{vmatrix}$$

and $D_r, r = 1, 2, 3$ is determined, as before by replacing the rth column of $|c|$ by a column k 's. Also

$$\begin{aligned} c_{11} &= d_1 & c_{21} &= c_1 & c_{31} &= t_1 & k_1 &= \cos \gamma \\ c_{12} &= d_2 & c_{22} &= c_2 & c_{32} &= t_2 & k_2 &= \cos 2\gamma \\ c_{13} &= d_3 & c_{23} &= c_3 & c_{33} &= t_3 & k_3 &= 0 \end{aligned}$$

Vector \bar{s} , normal to \bar{e} , \bar{t}

$$\bar{s} = \bar{e} \times \bar{t} = \begin{vmatrix} \bar{i} & \bar{j} & \bar{k} \\ e_1 & e_2 & e_3 \\ t_1 & t_2 & t_3 \end{vmatrix}$$

$$= s_1 \bar{i} + s_2 \bar{j} + s_3 \bar{k} \quad (51)$$

and

$$s = \sqrt{s_1^2 + s_2^2 + s_3^2} \quad (52)$$

so

$$\bar{s} = \frac{\bar{s}}{s} = s_1 \bar{i} + s_2 \bar{j} + s_3 \bar{k} \quad (53)$$

Plane ϕ_{cd} containing \bar{c}, \bar{d}

$$\phi_{cd} = t_1 x + t_2 y + t_3 z = d_{cd} \quad (54)$$

where

$$d_{cd} = t_1 x_1 + t_2 y_1 + t_3 z_1 \quad (55)$$

and where (x_1, y_1, z_1) are the coordinates of the point of intersection of the ray \bar{c} with the hyperboloid.

Plane ϕ_{te} containing \bar{t}, \bar{e}

$$\phi_{te} = s_1 x + s_2 y + s_3 z = d_{te} \quad (56)$$

where

$$d_{te} = s_1 x_1 + s_2 y_1 + s_3 z_1 \quad (57)$$

Plane ϕ_F containing the focal plane

$$\begin{aligned} \phi_F &= f_1 x + f_2 y + f_3 z \\ &= f_2 y = y = d_f \end{aligned} \quad (58)$$

where

$$d_f = y_2 \quad (59)$$

and y_2 is the coordinate of the focal plane.

Intersection of the re-reflected ray \bar{e} with the focal plane

The controlling equations for finding the pierce of \bar{e} in the focal plane are:

$$s_1 x + s_2 y + s_3 z = d_{te} \quad (60)$$

$$t_1 x + t_2 y + t_3 z = d_{cd} \quad (61)$$

$$y = y_2 \quad (62)$$

so

$$x = x_2 = \frac{D_1}{|d|}, \quad z = z_2 = \frac{D_2}{|d|} \quad (63)$$

where

$$|d| = \begin{vmatrix} d_{11} & d_{12} \\ d_{21} & d_{22} \end{vmatrix}, \quad D_1 = \begin{vmatrix} t_1 & d_{12} \\ t_2 & d_{22} \end{vmatrix},$$

$$D_2 = \begin{vmatrix} d_{11} & t_1 \\ d_{21} & t_2 \end{vmatrix} \quad (64)$$

and where

$$\begin{aligned} d_{11} &= s_1 & d_{21} &= t_1 & l_1 &= d_{te} - s_{2y} \\ d_{12} &= s_3 & d_{22} &= t_3 & l_2 &= d_{cd} - t_{2y} \end{aligned}$$

Thus the pierce point (x_2, y_2, z_2) of the ray \bar{e} with the focal plane is now known.

Radius of the pierce point in the focal plane, r_t

$$r_t = \sqrt{x_2^2 + z_2^2} \quad (65)$$

Figures 4-8 show the image size and shape having been reflected from points on the paraboloid having radii from the axis of symmetry $r_p = 2, 12, 22, 32$ and 42 feet, respectively. It is seen that the image shapes are not circular, but are not severely distorted from a circular shape. This is in contrast to the images cast by the sun, from points on the paraboloid, to a flat plate oriented perpendicular to the axis of symmetry and placed at the focus of the paraboloid at low angles of incidence.

Concentration ratio

Writing an identity for the energy arriving at the image, gives

$$\pi(r_p^2 - r_h^2) S_c \rho_p \rho_h = \pi r_{tm}^2 S_t \quad (66)$$

and defining

$$C_{av} = \frac{S_t}{S_c} = \frac{(r_p^2 - r_h^2)}{r_{tm}^2} \rho_p \rho_h \quad (67)$$

where

- S_c = solar constant
- S_t = average flux across the image at the focal plane
- r_p = radius of paraboloid considered
- r_h = radius of necessary hyperboloid
- $\rho_p \rho_h$ = hemispherical reflectivity of paraboloidal surface and hyperboloidal surface, respectively (averaged)
- r_t = radius of ray pierce point in the focal plane measured from the focal point of the hyperboloid
- r_{tm} = maximum radius of ray pierce point, considering the entire paraboloid

We may also write

$$C_{av} = C_i \eta_e \quad (68)$$

where

$$C_i = \frac{(r_p^2 - r_h^2)}{r_{tm}^2} = \text{ideal concentration (geometric)} \quad (69)$$

and

$$\eta_e = \rho_p \rho_h = \text{combined reflectivity factor} \quad (70)$$

The concentration above may be increased using a compound paraboloidal concentrator (or a cone can be used with less effectiveness) (2) according to

$$C_{cpc} = \frac{1}{\sin^2 \zeta} = \text{concentration by compound paraboloidal concentrator} \quad (71)$$

and

$$C_{aug} = C_{cpc} C_{av} = \text{concentration augmented} \quad (72)$$

where from Figure 9

$$\zeta = \tan^{-1} \left(\frac{r_t + r_h}{F + y_1} \right) \quad (73)$$

Thus

$$\begin{aligned} C_{aug} &= C_{cpc} C_i \eta_e = \\ &= \frac{(r_p^2 - r_h^2)}{r_{tm}^2} \frac{\rho_p \rho_h}{\sin^2 \zeta} \end{aligned} \quad (74)$$

and

$$\begin{aligned} C_{aug_i} &= C_{cpc} C_i = \frac{C_{aug}}{\eta_e} = \\ &= \text{ideal augmented concentration} \end{aligned} \quad (75)$$

Figure 10 shows a plot of the ideal concentration, C_i vs. the eccentricity e , for various values of CL, the distance from the vertex of the paraboloid to the focal plane (see Figure 1).

Figure 11 shows a plot of the ideal augmented concentration, C_{aug_i} vs. the eccentricity e , for various values of CL.

Figure 12 shows a plot of the necessary radius of the hyperboloid, r_h vs. the eccentricity e , for various values of CL.

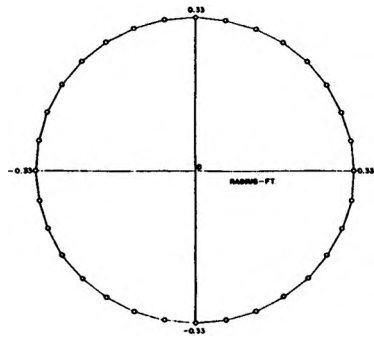


Fig. 4 Image Shape, $r_p = 2$ feet

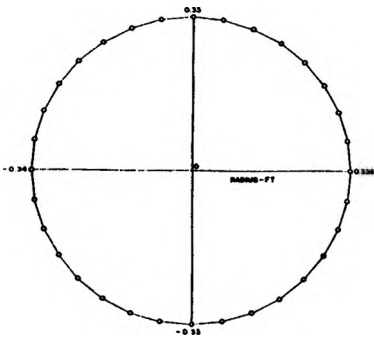


Fig. 5 Image Shape, $r_p = 12$ feet

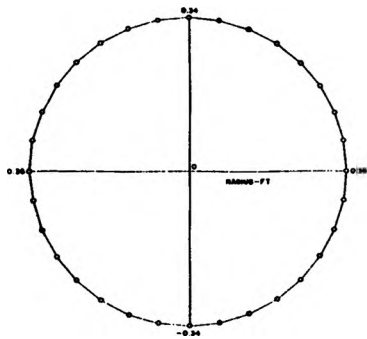


Fig. 6 Image Shape, $r_p = 22$ feet

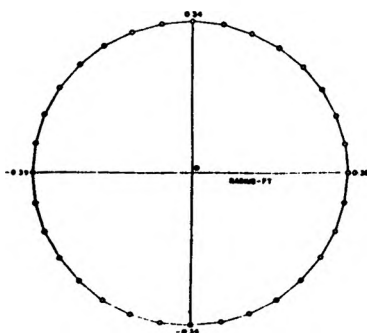


Fig. 7 Image Shape, $r_p = 32$ feet

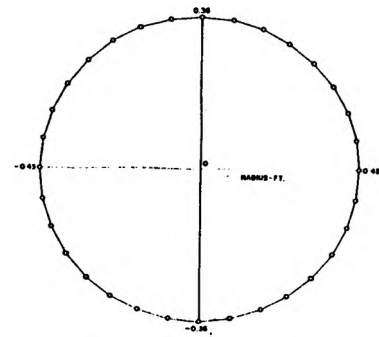


Fig. 8 Image Shape, $r_p = 42$ feet

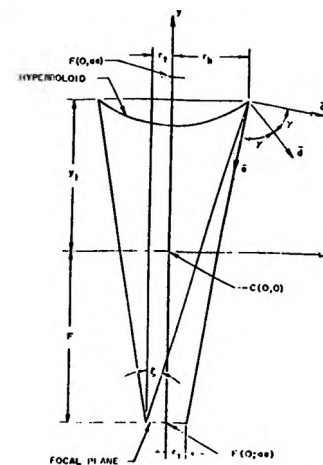


Fig. 9 Hyperboloid and Image Geometry

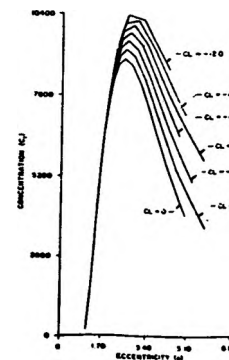


Fig. 10 Ideal Concentration vs. Eccentricity

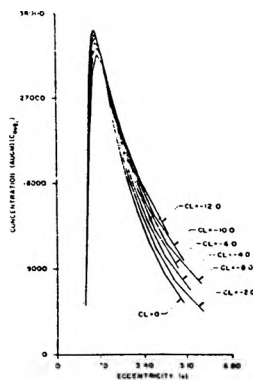


Fig. 11 Ideal Augmented Concentration vs. Eccentricity

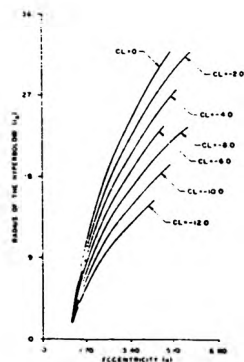


Fig. 12 Hyperboloid Radius vs. Eccentricity

NOMENCLATURE

$\bar{A}, \bar{B}, \bar{D}, \bar{P}, \bar{R}$

\bar{T}, \bar{S} = vectors

$\bar{a}, \bar{b}, \bar{c}, \bar{d}, \bar{e},$

$\bar{p}, \bar{r}, \bar{t}, \bar{s}$ = normalized vectors

$|a|, |b|,$

$|c|, |d|$ = determinants

a_0 = paraboloid constant

a, b = hyperboloid constants

BB_1, BB_2

BB_3, BB_4 = constants

$C_{av}, C_i, C_{aug},$

C_{cpc}, C_{aug_i} = concentrations

CL = distance from the vertex of the paraboloid to the focal plane

$d_{ab}, d_{cd},$
 d_{cp}, d_{te} = constants

D_r = determinant

f_0 = focal length of paraboloid

e = eccentricity

$F = ae$

$F(y), \bar{F}(y)$ = functions of y

$\bar{i}, \bar{j}, \bar{k}$ = unit vectors

k_r, l_r = constants

r = radius

r_h = radius of hyperboloid

r_p = radius of paraboloid

r_t = radius of ray pierce point in the focal plane measured from the focal point of the hyperboloid

r_{tm} = maximum radius of any ray pierce point considering the entire paraboloid

S_c = solar constant

S_t = average flux across the image at the focal plane

x, y, z = coordinates

α_s = angle subtended by the sun = 0.009322 radians

γ, θ, ζ = angles

∇ = gradient operator

$\phi_{ab}, \phi_{cd}, \phi_{cp},$

ϕ_{te}, ϕ_F = planes

REFERENCES

1. Cobble, M.H., Hull, W.C. and Hays, R.A., Analysis of a Cassegrain Solar Furnace, Proceedings, Vol. 161, Society of Photo-Optical Instrumentation Engineers, in press.
2. Rabl, Ari, Optical and Thermal Analysis of Concentrators, Solar Thermal Concentrating Collector Technology Symposium, p. 33, Denver, June 14 and 15, 1978.
3. Cobble, M.H., and Thacher, E.F., Verification of Wedge Concentration Using Argon Laser, Proceedings of the 24th Annual Technical Meeting, Institute of Environmental Sciences, in press.

BIOGRAPHIES

Dr. Cobble is Professor of Mechanical Engineering at New Mexico State University. He received his Ph.D. from the University of Michigan in 1958. He has published in the areas of heat transfer, fluid mechanics and solar energy.

Dr. Hull received his Ph.D. from the University of Toledo in 1975. He is an Associate Professor of Mechanical Engineering at New Mexico State University. He has published in the areas of fatigue and failure analysis, and solar furnace design.